

This work was written as part of one of the author's official duties as an Employee of the United States Government and is therefore a work of the United States Government. In accordance with 17 U.S.C. 105, no copyright protection is available for such works under U.S. Law.

Public Domain Mark 1.0

<https://creativecommons.org/publicdomain/mark/1.0/>

Access to this work was provided by the University of Maryland, Baltimore County (UMBC) ScholarWorks@UMBC digital repository on the Maryland Shared Open Access (MD-SOAR) platform.

Please provide feedback

Please support the ScholarWorks@UMBC repository by emailing scholarworks-group@umbc.edu and telling us what having access to this work means to you and why it's important to you. Thank you.

ESTIMATING REFLECTED AND EMITTED COMPONENTS OF THE RADIATION BALANCE USING REMOTELY-SENSED SPECTRAL DATA FROM KUREX-91

B. L. Blad, E. A. Walter-Shea, M. A. Mesarch and C. J. Hays
Department of Agricultural Meteorology
243 L. W. Chase Hall
University of Nebraska-Lincoln
Lincoln, NE 68583-0728

D. Deering and T. Eck
Code 923
Building 16W
NASA/Goddard Space Flight Center
Greenbelt, MD 20771

Abstract¹

The paper describes the estimation of incoming and outgoing radiation streams using bidirectional spectral reflectances and bidirectional thermal emittances. Good agreement between measured and modeled estimates of the radiation balance was obtained. Data used in this study were collected over selected grassland sites on the Streletskaya Steppe Reserve in Russia in July 1991. Results from this study compare well with results obtained during the FIFE study in Kansas in 1987-89.

Introduction

Net radiation (R_n), the balance of shortwave and longwave radiation streams, is the fundamental quantity of energy available at the earth's surface to drive the processes of photosynthesis, evaporation of water, and heating of the soil and air. Net radiation will vary spatially and temporally. It can be measured at specific locations with net radiometers, but since it is strongly influenced by the surface over which it is measured, it is difficult to extend measurements made at a specific location to other sites, especially if the surfaces are heterogeneous. Remote sensing offers the potential to provide estimates of R_n over different types of surfaces and over areas of various size.

Satellites and other remote sensing instruments do not measure the total hemispherical reflectance or hemispherical emittance directly. Therefore, it is necessary to develop algorithms and techniques to estimate hemispherical reflectances and emittances using spectral data collected by remote sensors. The primary objective of this study is to estimate hemispherical reflectances and hemispherical emittances from grassland surfaces using spectral bidirectional reflectances and bidirectional thermal emittances and to combine these estimates with incoming radiation streams estimated remotely or from readily available weather data to produce reliable estimates of net radiation.

Materials and Methods

The experiment was conducted on the Streletskaya Steppe Reserve in Russia in July 1991. Data reported here were taken almost exclusively from two grassland sites—a site mowed in 1989 but not in 1990 or 1991 (site 12), and one which had not been mowed for several years (site 14).

Bidirectional reflectance data were obtained with the Goddard PARABOLA instrument ([1] Deering and Leone, 1986) which measured radiation in the 0.650-0.670, 0.810-0.840 and 1.620-1.690 μm waveband region. For this study, only the reflectance data in the solar principal plane were used. From this principal plane reflectance data the method of [2] Walthall et al. (1985) was used to simulate directional hemispherical reflectance. The SPECTRAL 2 model developed by [3] Bird and Riordan (1984) was used to develop weighting coefficients to extend the spectral data collected by the PARABOLA to the entire solar spectrum. The approach of [4] Starks et al. (1991) was then used to combine the directional-hemispherical reflectance with weighting coefficients to produce an estimate of the surface albedo.

Bidirectional thermal emittances were determined with the Scheduler Plant Stress Monitor, a hand-held infrared thermometer (IRT). Readings were taken facing the four cardinal compass points in five 2 m x 2 m plots at each site. The IRT was held at an angle of about 45° approximately 1.5 m above the soil surface, and three readings were taken for each direction. The outgoing

longwave radiation was calculated using the average of the 12 IRT temperatures taken per plot. [5] Vining and Blad (1990) showed that good estimates of outgoing longwave radiation can be obtained from IRT readings made at a 40° view zenith angle.

The incoming shortwave radiation was estimated using the procedure described above for estimating albedo except that the reflected radiation was obtained over a BaSO_4 reference panel. The incoming longwave radiation was estimated using the model of [6] Brunt (1932). Several different equations available in the literature for estimating incoming radiation were tested against measured incoming longwave radiation in this study and the FIFE study ([7] Starks, 1990). Of all those equations the Brunt model did best here and in the FIFE study.

Each component of the radiation balance was measured using instruments mounted on an A-frame which was moved from site to site and/or from instruments mounted on the SERBS system operated by Dr. Leo Fritschen. For comparison with modeled estimates of incoming and reflected solar radiation measured values of these two radiation streams were obtained from Eppley Precision Spectral Radiometers (PSP) operated by Dr. Don Deering in association with PARABOLA measurements. Incoming and outgoing longwave radiation was measured with Eppley Precision Infrared Radiometers (pyrgeometer) model PIR(1). Net radiation was measured with REBS net radiometers. Instruments were typically mounted 1-1.5 m above the top of the vegetation.

Results & Discussion

The approach suggested by [4] Starks et al. (1991) was used to estimate the incoming solar radiation flux density. Modeled values are compared with measured values in Figure 1. The results show good agreement between the measured and modeled values, with a tendency for the model to overestimate the flux density of solar radiation, especially at flux densities below about 500 Wm^{-2} . Statistics for this comparison are shown in Table 1.

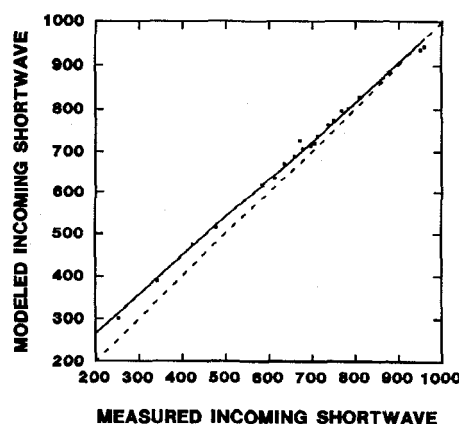


Figure 1. Flux densities of incoming solar radiation estimated with the model of [4] Starks et al. (1991) compared with measured values. The dashed line is the 1:1 line.

¹This work was supported by the National Aeronautics and Space Administration under Grant Nos. NAG5-1762 and NAG5-894.

The reflected shortwave radiation stream was estimated with the approach of [4] Starks et al. (1991) using the PARABOLA principal solar plane data. Estimated values are compared with measured values in Figure 2. As shown by the statistics given in Table 2 there was good agreement between the measured and modeled values but there was a definite trend for the modeled values to be greater than measured values.

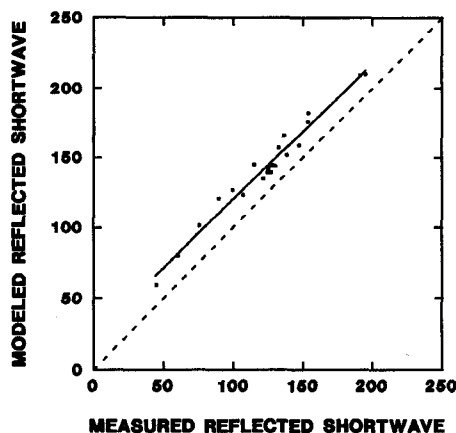


Figure 2. Flux densities of reflected solar radiation estimated with the model of [4] Starks et al. (1991) compared with measured values. The dashed line is the 1:1 line.

Data shown in Figures 1 and 2 were used to calculate the albedo of the surface with the results given in Figure 3 and Table 3. Modeled values tended to be higher than measured albedo by about 2% with a mean relative error of about 11%. These findings are similar to those reported by [4] Starks et al. (1991) for the data collected during the FIFE study. Possible reasons as to why modeled albedos are higher than measured ones was suggested by [4] Starks et al. (1991) and will not be repeated here.

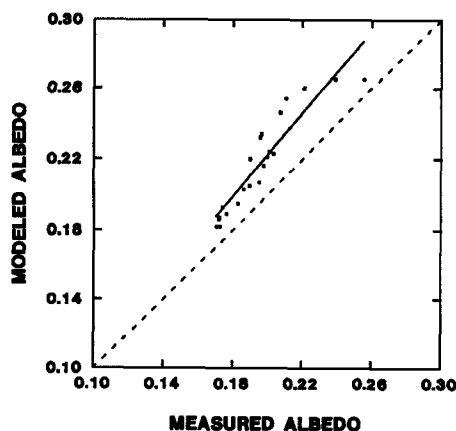


Figure 3. Albedo values calculated from incoming and reflected solar flux densities obtained with the [4] Starks et al. (1991) model compared with measured values. The dashed line is the 1:1 line.

The outgoing longwave radiation stream was estimated with the average IRT temperature obtained at the 45° view zenith angle and compared with the measured outgoing longwave radiation stream. Results are shown in Figure 4 and Table 4. There is very good agreement between the measured and estimated values especially at flux densities between about 375 and 450 Wm^{-2} .

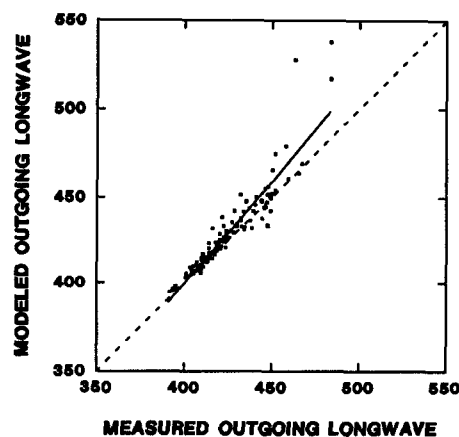


Figure 4. Flux densities of outgoing longwave radiation estimated from average canopy temperatures measured with an IRT (Scheduler) at a 45° view zenith angle compared with measured values. The dashed line is the 1:1 line.

The incoming longwave radiation stream estimated with the [6] Brunt (1932) equation is compared with the measured stream in Figure 5. There is good agreement between measured and modeled values. Statistics for the comparison of estimates of incoming longwave radiation estimated by the Brunt and other models are given in Table 5. The Brunt model gave the best estimates of incoming longwave radiation but the modified Deacon and modified Swinbank models also worked quite well.

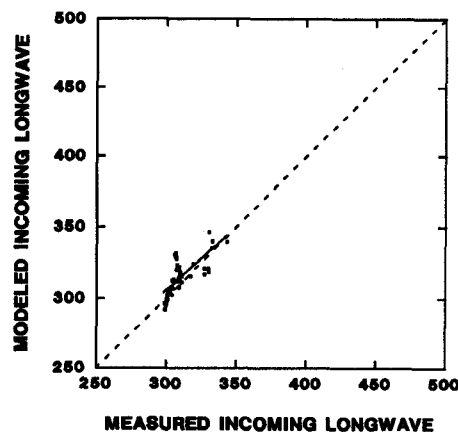


Figure 5. Flux densities of incoming longwave radiation estimated with the Brunt equation compared with measured values. The dashed line is the 1:1 line.

All estimated components of the radiation balance discussed above were combined to give an estimate of R_n . The estimated R_n was then compared with R_n measured on the A-frame (Figure 6). There is excellent agreement between estimated and modeled values as shown by the comparison statistics given in Table 6. It is interesting to note that the R_n estimated using the procedures described above agreed better with the measured R_n than when the radiation balance was calculated using measured components of each incoming and outgoing radiation stream (Table 6). The reason for the better agreement of the estimated R_n and the component calculated R_n with measured R_n is not certain, but is probably related to the fact that most of the measured components were made at different locations than the place where the R_n was measured. In the FIFE study the calculation of R_n using measured components agreed better with measured R_n than did the R_n estimated using the models similar to those in this study. There was better agreement between measured and estimated R_n in the KUREX-91 study than was found in the FIFE study.

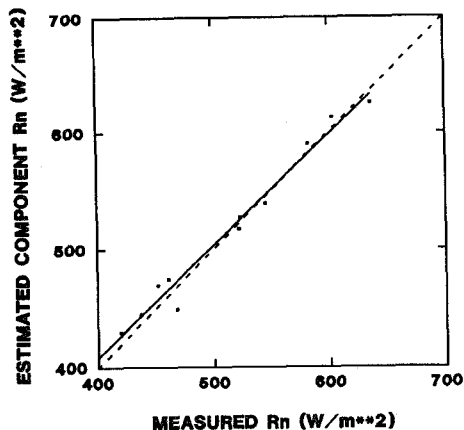


Figure 6. Flux densities of net radiation estimated from the radiation balance components in Figures 2-6, compared with R_n measured with the REBS net radiometer on the A-frame. The dashed line is the 1:1 line.

Conclusions

The algorithms and procedures developed and/or tested in FIFE to estimate R_n and its component parts worked very well for estimating the flux densities of incoming and outgoing radiation and net radiation in the KUREX-91 study. In fact, they actually produced better estimates when compared to measured values than was observed for the FIFE data. The results of these studies suggest that R_n can be reliably estimated using remote sensing techniques.

References

- [1] D. W. Deering and P. Leone, "A sphere-scanning radiometer for rapid directional measurements of sky and ground radiance," *Remote Sensing Environment*, Vol. 10, pp. 1-24, 1986.
- [2] R. Bird and C. Riordan, Simple solar spectral model for direct and diffuse irradiance on horizontal and tilted planes at the earth's surface for cloudless atmospheres. Solar Energy Research Institute, Golden, CO, 1984, 1984.
- [3] C. L. Walthall, J. M. Norman, J. M. Welles, G. Campbell and B. L. Blad, "Simple equation to approximate the bidirectional reflectance from vegetative canopies and bare soil surfaces," *Applied Optics*, Vol. 24, pp. 383-387, 1985.
- [4] P. J. Starks, J. M. Norman, B. L. Blad, E. A. Walter-Shea and C. L. Walthall, "Estimation of shortwave hemispherical reflectance (albedo) from bidirectionally reflected radiance data," *Remote Sensing Environment*, Vol. 38, pp. 123-134, 1991.
- [5] R. C. Vining and B. L. Blad, "Relationship between radiometric, aerodynamic and kinetic canopy temperatures of prairie vegetation," *Proceedings of the Symposium on FIFE*, p. 106, American Meteorological Society, 1990.
- [6] D. Brunt, "Notes on radiation in the atmosphere 1," *Quart. J. Roy. Meteorol. Soc.*, Vol. 58, pp. 389-418, 1932.
- [7] P. J. Starks, *Measured and modeled radiation fluxes*. Ph.D. Dissertation, University of Nebraska, 1990, 179 pp.

Table 1. Statistics from comparison of incoming shortwave estimations with measured Eppler incoming shortwave longwave values from Deering using the KUREX91 dataset. $N=22$.

Algorithm	d	r	r^2	MBE Wm^{-2}	MRE %	RMSE Wm^{-2}	E_u Wm^{-2}	E_s Wm^{-2}	\bar{x} Wm^{-2}	\bar{s} Wm^{-2}	cv
modelled	0.99	1.00	1.00	25.89	5.95	31.88	10.50	30.10	709.70	182.79	0.26
measured									648.24	205.00	

where

$$d = 1 - [\Sigma(E-M)^2 / \Sigma E \cdot x + (M-x)^2]$$

E = estimated value
 M = measured value
 \bar{x} = mean measured value
 $RMSE = \{[(N-1)\Sigma(P-M)^2] + [N^{-1}\Sigma(P-E)^2]\}^{1/2}$
 $E_s = (N^{-1}\Sigma(P-M)^2)^{1/2}$
 $E_u = (N^{-1}\Sigma(P-E)^2)^{1/2}$
 P = predicted value from linear regression of estimated and measured values
 $MBE = N^{-1}\Sigma(E-M)$
 $MRE = N^{-1}[\Sigma(E-M)/M][100]$
 $\bar{x} = N^{-1}\Sigma E$ or $N^{-1}\Sigma M$
 $\bar{s} = [(N-1)^{-1}\Sigma(E-x)^2]^{1/2}$ or $[(N-1)^{-1}\Sigma(M-x)^2]^{1/2}$
 $cv = \bar{s}/\bar{x}$

Table 2. Statistics from comparison of reflected shortwave estimations with measured Eppler reflected shortwave values from Deering using the KUREX91 dataset. $N=22$.

Algorithm	d	r	r^2	MBE Wm^{-2}	MRE %	RMSE Wm^{-2}	E_u Wm^{-2}	E_s Wm^{-2}	\bar{x} Wm^{-2}	\bar{s} Wm^{-2}	cv
Walthall	0.92	0.98	0.97	19.45	17.71	20.47	6.28	19.48	152.02	36.03	0.24
measured									123.77	36.00	

Table 3. Statistics from comparison of albedo estimations with measured Eppley albedo values from Deering using the KUREX91 dataset. N=22.

Algorithm	d	r	r ²	MBE	MRE %	RMSE	Eu	Es	x	s	cv
Walthall	0.78	0.93	0.86	0.022	11.085	0.025	0.010	0.023	0.218	0.026	0.119
measured									0.196	0.022	

Table 4. Statistics from comparison of outgoing longwave estimations from the average of the Scheduler 45° surface temperature measurements changed to units of Wm⁻² with measured pyrgeometer outgoing longwave values using the KUREX91 dataset.

Algorithm	d	r	r ²	MBE Wm ⁻²	MRE %	RMSE Wm ⁻²	Eu Wm ⁻²	Es Wm ⁻²	x Wm ⁻²	s Wm ⁻²	cv
modelled	0.94	0.93	0.87	4.50	1.02	10.28	8.60	5.63	430.16	24.00	0.06
measured									425.66	18.89	

Table 5. Statistics from comparison of various incoming longwave estimations with measured pyrgeometer incoming longwave values using the KUREX91 dataset. N=55.

Algorithm	d	r	r ²	MBE Wm ⁻²	MRE %	RMSE Wm ⁻²	Eu Wm ⁻²	Es Wm ⁻²	x Wm ⁻²	s Wm ⁻²	cv
Brunt	0.82	0.74	0.55	4.72	1.53	9.26	9.01	2.13	314.97	12.74	0.04
Swinbank	0.33	0.63	0.40	42.28	11.04	41.80	9.02	40.81	350.94	14.35	0.04
mod. Swinbank	0.66	0.63	0.40	10.68	3.46	15.51	11.04	10.90	320.94	14.35	0.04
Deacon	0.35	0.63	0.40	38.83	10.97	38.33	9.02	37.25	347.25	14.26	0.04
mod. Deacon	0.72	0.63	0.40	7.24	2.35	13.23	10.97	7.40	317.49	14.26	0.04
measured									310.26	10.63	0.03

Table 6. Statistics from comparison of Rn from estimated components (reflected shortwave-Walthall model, incoming longwave - Brunt model, outgoing longwave average of 45° Scheduler), measured components (incoming and reflected shortwave - Deering data, incoming longwave Fritschen data, outgoing longwave A-frame data), measured by the REBS net radiometer on the A-frame.

Method	d	r	r ²	MBE Wm ⁻²	MRE %	RMSE Wm ⁻²	Eu Wm ⁻²	Es Wm ⁻²	x Wm ⁻²	s Wm ⁻²	cv
Measured components	0.98	0.97	0.95	4.59	0.63	26.54	25.81	6.16	508.30	91.68	0.18
Estimated components	0.99	0.99	0.98	3.82	0.92	23.12	19.37	12.64	507.52	72.82	0.14
measured									503.71	77.08	0.15